Project

Yuval Toren,

Submitted to Prof. Yakov Krasik and Mr. Daniel Shafer

February 2014

Table of Contents

1. Introduction

The purpose of the experiment is to measure directly the pressure at the vicinity of the axis of implosion a cylindrical converging strong shock wave generated by underwater electrical wire explosion.

The main idea behind electrical wire explosions is a rapid deposition of energy (characterized by discharge current density in the range of $10^6 - 10^{10}\left[{}^{A}/_{cm^2}\right]$, energy of several ${}^{kJ}/_{g}$, Pressure of up to $10^5\left[\text{kK}\right]$ and pressure of up to $10^{10}\left[\text{Pa}\right]$) into wires within a very short time scale (usually $10^{-9} - 10^{-5}\text{s}$).

Electrical wire explosion was first discovered more than 200 years ago but has been subject of intense theoretical and experimental research for more than 50 years due to many important technical applications such as thermonuclear fusion, solid-state and plasma-chemical physics, rockets, generation of extremely powerful radiation ranging from infra-red to soft x-rays, strong shock waves and creation of nano-particles And also because of wide range of physical phenomena, such as the fast phase transitions of the exploding wire material: solid to liquid then it vaporizes and from vapor matter it become plasma. The plasma generated during this process is plasma of non-ideal, strongly coupled type, which is characterized by a coupling parameter $\Gamma = \frac{Z^2 e^2}{aK_B T} \geq 1$

(Where Z is the plasma ionization factor , e is the electron charge , $K_B T$ is the thermal energy of a particle and $a = \left({}^{3}/_{4}\pi n_i\right)^{1/3}$ is the average distance between the

particles of the plasma , where n_i is the plasma density) which represents the ratio between coulomb and thermal energies of interacting particles in plasma. If $\Gamma \gg 1$it means the plasma is of a strongly coupled type which means the coulomb energy is much greater than the thermal energy in the plasma, this kind of plasma is also characterized as relatively cold and dense. If $\Gamma \ll 1$ it means it is a weakly coupled plasma, where the thermal energy is much greater than the coulomb energy in the plasma, this type of plasma is characterized as hot and diffuse, in the case of weakly coupled plasma we can also say it is an ideal plasma which means one can refer to it as an ideal gas, and use everything known about ideal gasses. In order to achieve extreme state of matter, energy deposition rate into the wire has to be increased. Yet, in the case of electrical wire explosion in vacuum or gaseous environment, some phenomena reduce the deposited energy density, for example surface plasma flashover, which occur due to surface flash induced by induction voltage resulting in ionization of atoms and molecules released from the surface of the wire, and the subsequent formation of a current conducting, low density and fast expanding plasma shell which is called “corona”, the resistance of the shell is decreasing rapidly.
It leads to a deposit of a significant portion of the stored energy in the corona instead of depositing it in the wire. Hence, one of the methods of increasing the amount of deposited energy into the wire is by withholding the surface flashover by submerging the wire into a medium which disrupt the expansion or stop it completely, such as water, transformer oil or pressurized gas. In the experiment the wires were submerged in distilled water which has high dielectric constant ($\varepsilon \sim 81$) and is almost

incompressible and therefore, it prevents the surface flashover and allows a lowering of the radial expansion velocity of the exploding wire from $10^7 \left[{}^{cm}/_{s} \right]$ in vacuum to less than $10^5 \left[{}^{cm}/_{s} \right]$, which results in high energy density deposition rate and value as well.

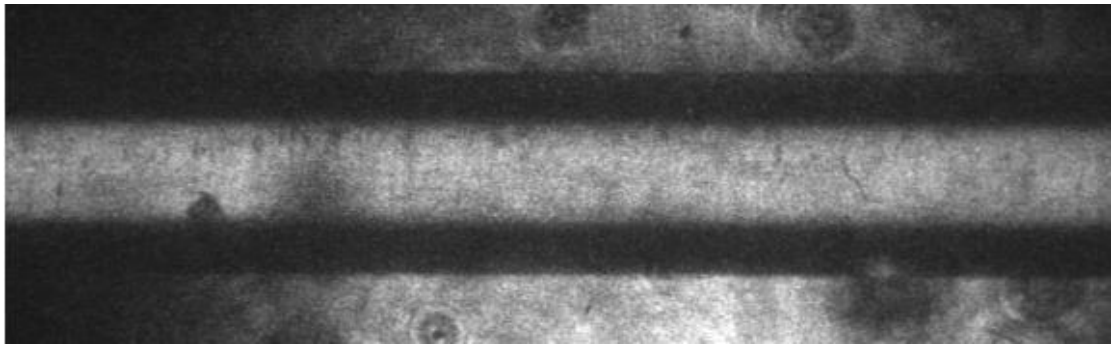

Figure 1: *Typical image of the self-light emission from the surface of the discharge channel and shadow image of expanding shock wave in water*

There are two approaches to underwater electrical wire explosion (UEWE): discharging through a thin wire of a few microns in diameter and discharging through a thick wire (diameter larger than a few microns).When a thin wire is used the wire explode very close to the beginning of the discharge and most of the stored energy is deposited into the water, the wire explosion serves as an igniter to the main discharge which occur through the ionized water vapor. Thus, such process is called underwater electrical discharge (UED). An important technological application of this process is a method of pressing parts with complex shapes by strong shock wave (SSW) resulting from the UED. When the exploding wire diameter is more than a few microns, most of the energy stored in the generator is deposited onto the wire and used for the wire explosion, the electrical discharge mainly occurs in the ionized material of the exploded wire. This kind of discharge is mostly determined by properties (diameter,

length and material) of the wire, rather than properties of the surrounding water or the formation and shape of the electrodes, hence this kind of discharge is called UEWE. In the experiment we used one of many applications of UEWE which is the generation of a converging SSW with a cylindrical wire array. In this configuration each wire generates its own SSW, which is an expanding cylindrical SSW, and they are combined with the SSWs of the neighboring wires, creating a strong, converging cylindrical SSW. This SSW is propagating towards the axis of implosion, creating tremendously high pressure, density and temperature (up to $5\times10^{11}[\mathrm{Pa}]$, $4\left[{}^{g}\!/_{cm^3}\right]$ and few eV respectively) of the water at the surrounding area of the axis of implosion. Electric parameters of the generator play an important role on the energy and density deposition rate. First, as already described, the maximum stored energy varies from generator to generator, and may also be changed by charging the same pulsed generator to different voltages. Second, the energy deposition rate depends on the typical rise time of the system which we can calculate with $\tau=\frac{\pi\sqrt{LC}}{2}$ (this is the typical rise time of the discharge current). And therefore there is a difference between UEWE experiments not only in wire parameters but also in the generator timescale which also implies to the UEWE timescale. There are significant differences in the conditions obtained at different timescales. In microsecond timescale, the temperature of the wire usually reaches up to $30\,\mathrm{kK}$. The typical skin depth for this timescale is larger than the wire radius and therefore, one can assume radial uniformity of the

current density flowing through the wire .Therefore, one can also assume the plasma column parameters are uniform.

2. Experimental Setup

2.1. General description of the experimental setup and experimental phases

The experimental system consists of two main parts: a generator and a measurement circuit. A Microsecond timescale pulsed-current generator based on four Maxwell-type high-voltage capacitors and four multigap gaseous switches was used for the explosion of 15mm and 11.5mm in radius cylindrical arrays of 40 Cu wires each of 0.1 mm diameter and 45mm (for the 15mm radius array) or 40mm (for the 11.5mm radius array) length. The wire array parameters were chosen in such way to obtain a-periodical discharge of the generator were most of the energy stored in the capacitors is transferred to the wire array to make an underwater electrical wire explosion.

The four multigap gaseous switches are triggered at the same time with a Marx generator.

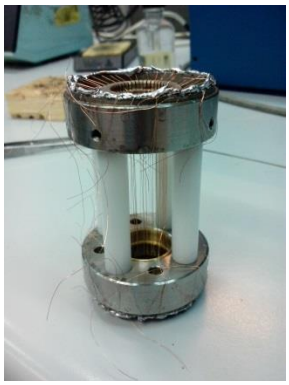

Figure 2: *The wire array*

With the wire array connected to the generator the total inductance is approximately $80[\mathrm{nH}]$. The generator was charged with a voltage of 27kV and with it the generator can produce a current with an amplitude of up to 300kA during UEWE (We charged it to 28kV to prevent fast weathering, the generator can hold up to 35kV) in approximately $1.2\mu s$ rise. In order to measure the pressure the converging shock wave creates at the axis of implosion, we used a measurement circuit which gets signals from a manganin wire placed at the shock wave's axis of implosion. In the measurement circuit there is a self-integrating rogowski coil to measure the current on the manganin an active voltage divider to measure the voltage on it and a spark gap to trigger the measurement at a fixed time (after the electromagnetic field from the generator decayed so it won't disturb the measurement). The wire array is connected to the pulsed-current generator a capacitive voltage divider which measure the voltage on the array and a self-integrating rogowski coil which measure the current flow through the array and is fixed horizontally inside a stainless steel container between the cathode and anode electrodes. The container is filled with distilled water (instead of regular tap water) to prevent breakdown through water. Breakdown through water means UED and in our experiment we want to create an UEWE which happens when the voltage is discharged mostly through the wire material and not it's surrounding. The whole experimental system is connected to two oscilloscopes (one connected to the generator and the other to the measurement circuit) which start to work when the trigger pulse is starting the process .The oscilloscopes get signals from two Rogowski

coils (current signals, from the array and the manganin), two voltage dividers one capacitive and one active (voltage signals, from the array and the manganin) and a CVR (current signal from the manganin).We also did a short circuit experiment, where the array was replaced with a metal rod to prevent UEWE and measuring the inductance and investigate the periodic voltage and current.

2.2. Microsecond pulsed-current generator

This generator is based on the concept of Pulsed discharge capacitor. The generator is built from four Maxwell-type high-voltage capacitors and four multigap gaseous switches for a synchronized discharge of the four capacitors to gain full power in the system. The total capacitance of the generator is approximately $10[\mu\mathrm{F}]$.

The main reason for using a generator based on high-voltage energy-storage capacitors is that building fast; reliable, repetitive, fast closing switches are easier to build than the opening switches necessary for generators based on inductive storage. Another reason is the fact that capacitors can hold energy for a much longer time than other energy storage practices, for example inductive storage devices. The stored energy in a capacitor is: $W_C = \frac{1}{2}CU^2$ Where U is the charging voltage and C is the capacitance which is defined as $C = \frac{\epsilon\epsilon_0 A}{d}$ where A is the area, ϵ is the relative dielectric constant ϵ_0 is the dielectric constant of the vacuum and d is the thickness of the dielectric matter. A lumped circuit model of a capacitor is illustrated as:

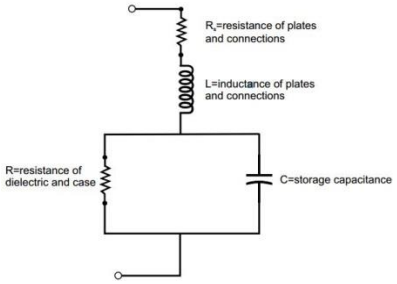

Figure 3: *Lumped circuit model of a capacitor*

The resistance represents the current leakage over the dielectric and the capacitor case. The inductance is associated with the arrangement of the capacitor and its size. The inductance is limiting the peak current one can extract from a capacitor by $I_{MP} = U\sqrt{\frac{C}{L}}$. When a capacitor is charged or discharged quickly its momentary capacitance is different from its static value. This phenomenon results from the finite relaxation time of the polarization, which is also responsible to the dielectric losses that occur in capacitors. The following illustration shows the generator circuit (without the 4 capacitors):

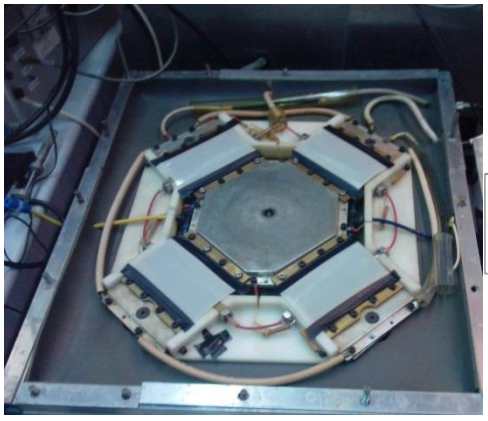

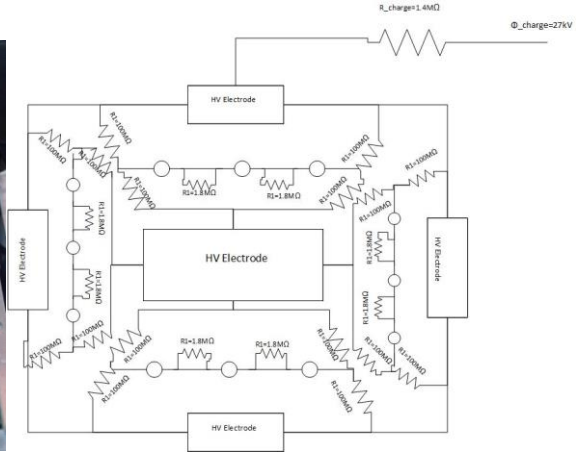

Figure 4: *from left to right – The microsecond timescale generator. The microsecond timescale generator circuit scheme*

2.3. Marx Generator

In the experiment we used a Marx generator as a part of the triggering circuit of the microsecond generator. The generator is triggering all four multigap gaseous switches at the same time in order to maximize the power invested in the wire array.

Commonly, Marx generators are used when one want to produce high-voltage pulses with an amplitude larger than 100kV. The underlying principle of this generator is to charge several capacitors in parallel and then discharge them in series formation, Hence the output voltage become:

$$V_{out} = \left(Number of\ capacitors \right) \times V_{in}$$

Figure 1 illustrates a simple Marx generator circuit with a uni-polar charger, where the capacitors are charged through the resistors R_L while the switches (triggers) are open:

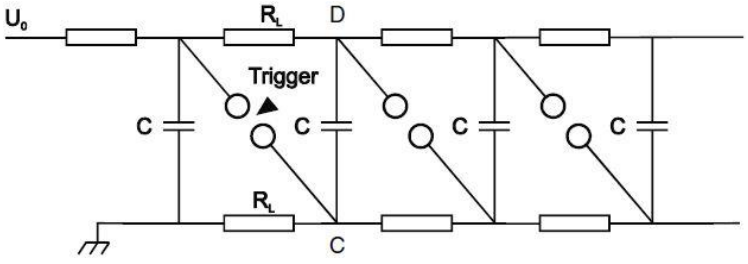

Figure 5: *Marx generator circuit with unipolar charging through the resistors* R_L

When the capacitors reach a high enough voltage, they discharge in series via spark gaps. The first spark gap is set narrower than the rest to encourage firing. When the first one fires, twice the voltage is implied on the next gap causing that one to fire. The gaps cascade and all the capacitors are now in series for a brief moment (The first gap can also be triggered manually). They then discharge through a load, or a big spark gap. The time for this process is usually of the order of microseconds. The impedance of Marx generator is $Z_M = \sqrt{\frac{L_M}{C_M}}$ .Because the capacitors are connected in series when the generator discharges we get that $L_M \propto nL$ and $C_M \propto \frac{C}{n}$, where n is the number of capacitors and we assume all of them are the same, Therefore the impedance $Z_M \propto n\sqrt{\frac{L}{C}}$. The smaller the impedance, the larger is the available power but since the impedance is growing linearly with the number of capacitors in the circuit there must be a balance between the number of capacitors and the impedance where one get the most out of the Marx generator for his needs. This is also the reason why it is difficult to raise the power of Marx generators to the level of terawatt and above and therefore the major role of Marx generators in ultra-high power generators is to pulse-charge an intermediate storage capacitors (water or oil).

2.4. Measuring instruments

In the experiment we used several measuring instruments to measure current and voltage on the manganin wire and on the wire array. In order to measure current we

used self-integrating rogowski coils and a current viewing resistor (CVR), and in order to measure voltage we used active and capacitive voltage dividers.

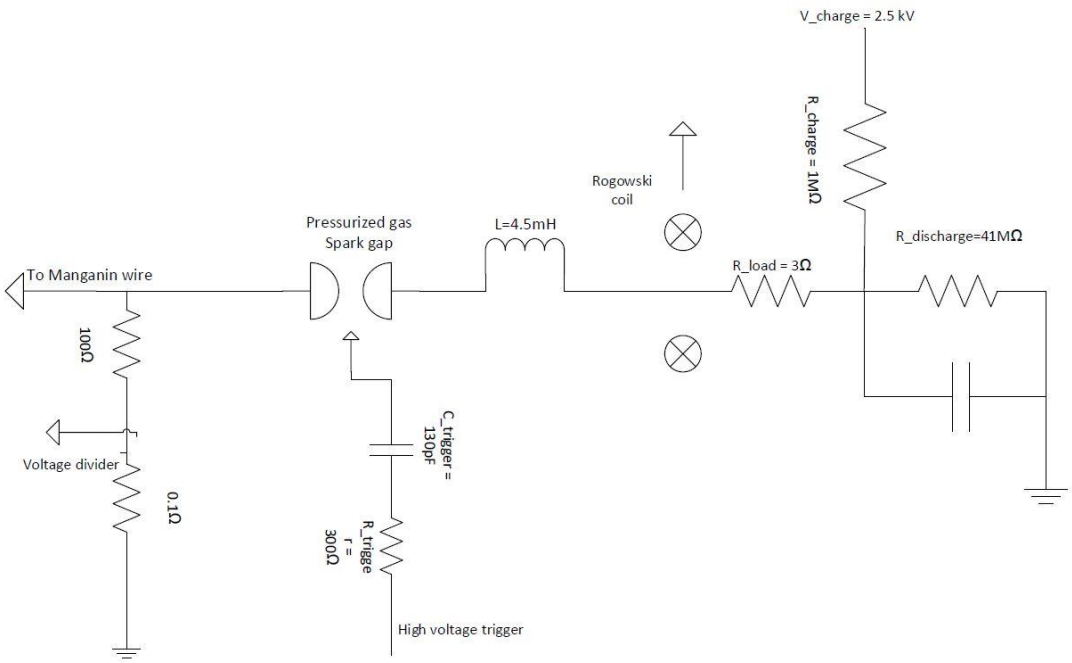

Figure 6: *The measuring circuit scheme*

There is one self-integrating rogowski coil connected to the manganin wire which measure the current flow to the manganin and one on the microsecond generator high voltage electrode which measure the current flow to the wire array. There is an active voltage divider connected to the manganin wire which measure the voltage applied on the manganin wire and a capacitive voltage divider connected directly to the wire array which is measuring the voltage applied on the wire array.

2.4.1. Current viewing resistor

In principle, the current viewing resistor is simply a low-value resistor. The current of interest is passing through the CVR and the potential across the CVR is recorded. The measured current is then calculated with $I_{CVR} = {}^{V_{CVR}}\!/_{R_{CVR}}$.

The resistance value of the CVR is selected such that the potential developed across the CVR resistance at full current may be considered sufficiently negligible that normal circuit operation is unaffected (i.e. it is a non-disturbing measurement).

The resistance of typical current-viewing resistors is often quite small ranging from several milliohms to μOhms. This low resistance creates two issues in the application of the CVR.

The first issue is series inductance in series with the CVR. Such inductance can be an unintended inductance introduced due to a not optimum implementation of the CVR, or it can be an inherent inductance in the CVR sensor. Series inductance results in a network zero in the frequency response of the CVR at $\omega_0 = {}^{R_{CVR}}\!/_{L_{CVR}}$. At frequencies above ω_0 , the impedance of the CVR rises linear with the frequency. This results in the output potential at frequencies above the response zero being higher than would be from the CVR resistance without it. The error can be quite significant, particularly for very low-value CVR devices. In this case we expect errors on the order of 1,000 to 10,000. Often the series inductance is unknown. As a result, very significant measurement errors can occur in pulsed-current measurements.

The low value of the CVR resistance can also result in instrumentation errors at DC and low frequencies below any response zero created by series inductance. This is due to parasitic resistance in the overall effective measurement path. This parasitic resistance is often not obvious, what causes it to be overlooked.

The effect of this parasitic resistance is to cause the output potential of the CVR to appear higher than that due to the CVR resistance alone. This error too can be quite significant, and ranges between factors of 10 to 1000. However, this error is due to the instrumentation configuration, and is not a characteristic of the CVR sensor.

2.4.2. Not integrating Rogowski coil

Not integrating Rogowski coil is an electrical device for measuring alternating current (AC) or high speed current pulses. It is made of a helical coil of wire with the lead from one end returning through the center of the coil to the other end, so that both terminals are at the same end of the coil. The whole assembly is then wrapped around the straight conductor whose current is measured. The theory of a Not integrating Rogowski coil is illustrating Ampere’s Law very well.

A Not integrating Rogowski coil works by sensing the magnetic field around the conductor and Ampère's Law provides the relationship between the current flowing and the magnetic field around it. If a line is drawn in a loop which totally encircles the current then, according to Ampère's Law, the line integral of the magnetic field around the loop is equal to the net current enclosed by it no matter what path the loop takes. If the loop encloses no net current the line integral is zero. Mathematically this

is expressed as $\oint \vec{H}d\vec{l} = I$ where dl is a small element of length along the loop, H is the magnetic field.

The Figure shows a helical coil, with n turns per meter and cross-sectional area A which encircles a conductor carrying a current I.

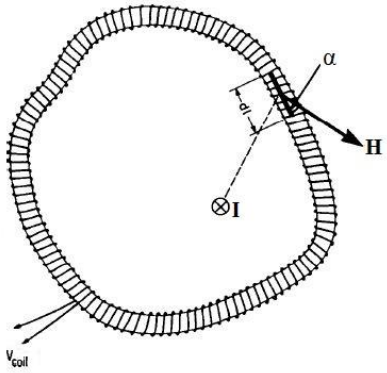

Figure 7: *Simple illustration of B – dot Principle of operation*

In a section of length dl the number of turns is ndl and the magnetic flux linking the section is

$$d\Phi = \mu_0 HAndl\cos(\alpha)$$

α Is the angle between the direction of H and the axis of the coil section. The flux linking the entire coil is given by integrating along the coil:

$$\Phi = \int d\Phi = \mu_0 nA\int H\cos(a)dl = \mu_0 nAI$$

We evaluated the integral with Ampère's law. For an alternating current the voltage output from the coil is given by the rate of change of flux:

$$V_{coil} = -\frac{d\Phi}{dt} = -\mu_0 An \frac{dI}{dt}$$

Ampère's Law makes a thin not integrating Rogowski coil ideal for use as a sensor for alternating currents since it responds only to currents which thread the loop and doesn't measure currents and fields from external sources. Also the output of the sensor does not depend on the path taken by the loop.

2.4.3. Self-integrating Rogowski coil

When one measures a current by the use of not integrating Rogowski coil an additional integration is required because straightforward measurement gives derivatives of the current self-magnetic field. One can measure the current directly by using a Rogowski coil in a self-integrating mode which means that $\frac{L}{R} \gg t_p$, where L is the inductance of the Rogowski coil and R is s the load resistance.

2.4.4. Active Voltage Divider

Voltage divider is a linear circuit that produces an output voltage which is a fraction of its input voltage. Voltage division is caused due to partitioning of a voltage among the components of the divider.

It is commonly used to create a reference voltage, or to get a low voltage signal proportional to the voltage to be measured. For direct current and relatively low frequencies, a voltage divider may be sufficiently accurate if made only of resistors. In systems frequency response over a wide range is required; the voltage divider may

have capacitive elements added to allow compensation for load capacitance. In electric power transmission, a capacitive voltage divider is used for measurement of high voltage.

A voltage divider referenced to ground is created by connecting two electrical impedances in series.

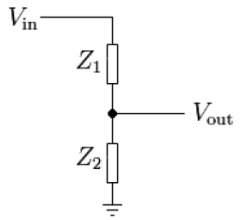

Figure 8: *Simple active voltage divider circuit scheme*

The input voltage is applied on the series impedances Z_1 and Z_2, the output is the Voltage on Z_2.

Z_1 And Z_2 can be built of any combination of resistors, inductors and capacitors.

Using Ohm's Law, the relationship between the input voltage and the output voltage is:

$$V_{out} = \frac{Z_2}{Z_1 + Z_2} V_{in}$$

There are several major requirements for voltage dividers:

A. A voltage divider should have a fast response (a broad bandwidth). In order to provide a broad bandwidth, the resistance of the high-voltage and low-voltage stages of an active voltage divider should be as small as possible in order to

provide a fast discharge (small RC) of stray capacitors to the ground. In the case of high frequencies this divider operates as a capacitive voltage divider because usually $\frac{1}{\omega t} \ll R$

B. An active voltage divider should have a large internal resistance which is much larger as compared with the plasma resistance.

C. In the case of the capacitive voltage divider one has to provide $RC \gg t_p$, where t_p the duration of the voltage pulse.

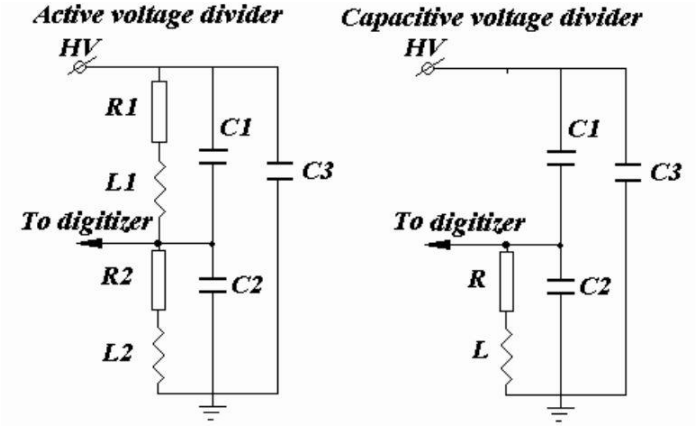

Figure 9: *Active and Capacitive voltage dividers circuit schemes*

2.5. The Manganin wire

2.5.1. About the manganin

Manganin gauges are an important tool for the direct measurement of high dynamic stresses. Measurements of stresses as high as 125 GPa have been reported. Manganin is a generic term for alloys consisting of 83 to 87% copper, 12 to 13% manganese and 0 to 4% nickel. The composition of the Manganin gauge is usually 84% copper, 12% manganese and 4% nickel. Manganin alloy has a large positive

piezoresistive coefficient, from 38 to 48 $\frac{\mu\Omega}{cm}$ and a low temperature resistivity coefficient, less than 15 $ppmi \times C$. The low temperature resistivity coefficient and the large piezoresistance coefficient of Manganin alloy mean that, when it is dynamically compressed, the change in resistance due to the induced stress is much larger than the accompanying change due to temperature. The qualities which make Manganin alloy a good material for use as a measurement instrument for dynamic stress measurements are: Resistance change from a short piece of Manganin alloy is large enough to be measured, and the fact that a Manganin wire may be made very thin and does not disturb the propagation of the shock wave and material flow. Stress measurements are conducted by monitoring the resistance change across the Manganin alloy caused by the dynamic load. This change is due to both the variation in dimensions and resistivity. At very high stresses (GP. region) involving uniaxial strain, the changes in the gauge dimensions are small so that the change in resistance is predominantly caused by the variation in resistivity.

2.5.2. The usage of Manganin in the experiment

In the Experiment we used Manganin in a wire configuration, which we connected to a measurement circle and place at the axis of implosion of the generated cylindrical shock wave. We used a wire configuration because it has a cylindrical symmetry, the same as the converging shock wave which means the stress will spread uniformly along the Manganin wire and hence the resistance will be homogeneous along the Manganin wire. We measured the current and voltage along the Manganin wire and

used ohm's law to determine the resistance of the wire, and from the resistance we could calculate the pressure at the axis of implosion.

3. Results and data analysis

The next step was analyzing the data from the oscilloscopes. In order to calculate the resistive voltage on the wire array, the voltage we applied directly on the wire array, we did a short circuit experiment to find it. we used $V(t=0)=L\left.\frac{dI}{dt}\right|_{t=0}$ and by comparing the voltage at the beginning of the short circuit experiment to the derivation in time of the current at the beginning of the short circuit experiment we got $L\approx 16[\mathrm{nH}]$ Which is the array inductance.

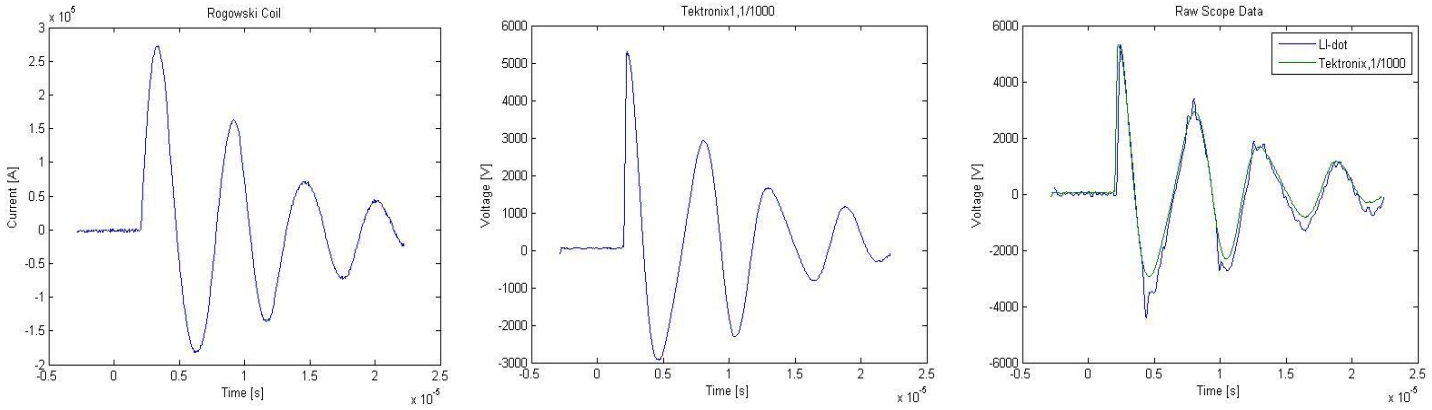

Figure 10: *from left to right – Typical wave form of the current of the microsecond generator at a short circuit experiment .Typical wave form of the voltage of the microsecond generator at a short circuit experiment. The inductive voltage and total voltage of the microsecond generator at a short circuit experiment*

We obtained the resistive voltage by using the inductance we found and the formula: $V_{total}=V_{resistive}+L\dot{I}$. The power is obtained with $P(t)=I(t)V(t)$ and the invested energy is gained through integrating the power in time.

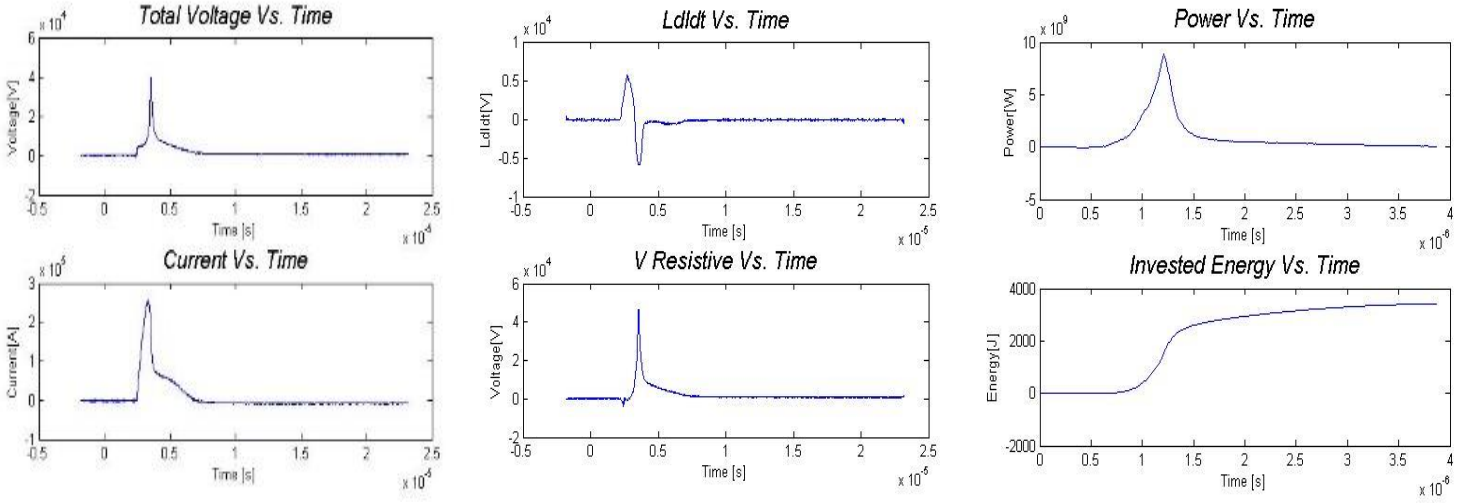

Figure 11: *from left to right: Typical waveforms of the current and total voltage of the microsecond timescale generator. Typical inductive voltage and resistive voltage of the microsecond generator with the wire array. The Power and the energy invested in the experiment.*

References

1. S. Efimov, A. Fedotov, S. Gleizer, V. Tz. Gurovich, G. Bazalitski, and Ya. E. Krasik. "*Characterization of converging shockwaves generated by underwater electrical wire array explosion*". Physics of plasmas **15** (2008).
2. H. Bluhm. "*Pulsed Power Systems*". Germany: Springer (2006).
3. G. Yiannakopoulos. "*A review of Manganin gauge technology for Measurements in the gigapascal range*". Australia (1990).
4. L. H. Dmowski and E. Litwin-Staszewska. "*The variation of the pressure coefficient of Manganin sensors at low temperatures* ". United Kingdom: Meas. Sci. Technol. **10** (1999).
5. D. Shafer, "*Investigation of Cu, Al and W conductivity during underwater wire explosion"*, M.Sc. Thesis, Israel (2011).
6. A. Fedotov, "*Underwater electrical wire explosion and shock wave generation in water"*, Ph.D. Thesis, Israel (2011).
7. Ya. E. Krasik, A. Grinenko, A. Sayapin, S. Efimov,A. Fedotov, V. Z. Gurovich, and V. I. Oreshkin, *"Underwater Electrical Wire Explosion and Its Applications"*, IEEE Transactions on plasma science, VOL. 36, NO. 2, (2008).
8. A. Fedotov, A. Grinenko, S. Efimov, and Ya. E. Krasik, *"Generation of cylindrically symmetric converging shock waves by underwater electrical explosion of wire array"*, Appl. Phys. Lett. 90 (2007).

9. M. E. Gruchalla, *"Current-viewing resistor validation and application"*, unpublished work (1986-2008).
10. D. A. Ward and J. La T. Exon, *"Using Rogowski-coils for transient current measurements"*, Engineering science and education journal (1993).
11. Ya. Krasik, *"Plasma diagnostics"*, Plasma Physics course, Lecture 12, Technion (2014).
12. W. B. Thompson, *"An introduction to plasma physics"*, Great Britain, Pergamon Press (1962).
13. G. Bazalitski, V. Ts. Gurovich, A. Fedotov-Gefen, S. Efimov, Ya. E. Krasik, *"Simulation of converging cylindrical GPa-range shock waves generated by wire array underwater electrical explosions"*, Shock Waves, Volume 21, Issue 4 (2011).